Mechanical behaviour and physical ageing of semi-crystalline polymers: 3. Prediction of long term creep from short time tests

L. C. E. Struik*
Plastics and Rubber Research Institute TNO, PO Box 71, 2600 AB Delft, The Netherlands
(Received 29 March 1988; revised 18 October 1988; accepted 1 November 1988)

The effective time theory and linear-extrapolation method for predicting long term creep from tests of short duration developed earlier for amorphous polymers are generalized to semi-crystalline polymers. It is shown that the predictions are in good agreement with experiment.

(Keywords: semi-crystalline polymers; mechanical behaviour; ageing; creep)

INTRODUCTION

In reference 1, methods were described for the prediction of the long term creep of amorphous polymers from tests of short duration. These methods were derived theoretically from the empirical kinetics of creep and physical ageing. This last factor plays a role because, during long term creep, the material ages and continuously stiffens. In other words, the creep properties change with time (age) and this effect has to be incorporated in the prediction methods. The mathematical problems could be solved and the resulting prediction methods were tested experimentally. It turned out that reliable predictions are possible for extrapolations of up to a factor of 100–1000 on time scale. The methods were also generalized to long term stress relaxation and to dimensional instabilities (creep under the action of internal stresses)[1].

In parts 1 and 2 of the present sequence of papers[2,3], we showed that semi-crystalline polymers such as PP, HDPE, etc., are just as sensitive to physical ageing as the amorphous materials. Moreover, this ageing occurs below as well as above the conventional T_g of the material. This was explained by assuming a T_g distribution between a lowest value T_g^L and a highest value T_g^U (see Figure 1 of ref. 2).

Since ageing was shown to be the key factor in solving the prediction problem for amorphous materials[1], the finding of similar ageing phenomena in semi-crystalline polymers prompted us to verify whether the same or similar prediction methods can be used for the semi-crystalline materials. This turned out to be the case and the results of the study are described in the present paper. We begin with a recapitulation of the behaviour of amorphous polymers and with a brief description of the prediction methods developed earlier[1]. The generalization to semi-crystalline polymers is given next, together with the results of experiments undertaken to test the methods. As in references 2 and 3, we use the classification scheme of the four characteristic temperature regions: region 1 for $T < T_g^L$; region 2 for $T \sim T_g^L$; region 3 for $T_g^L < T < T_g^U$ and region 4 for $T \geqq T_g^U$. As shown in reference 2, the creep and ageing behaviour is typically different in these four regions. For information about the materials studied, refer to reference 2. Full details about the experimental techniques have been given in reference 1.

RECAPITULATION OF THE BEHAVIOUR OF AMORPHOUS POLYMERS

Ageing and short-time creep

An illustration of the creep behaviour of an amorphous glassy polymer ($T < T_g$) is given in *Figure 1*. As shown earlier[1], we can distinguish between two different types of behaviour.

Range I (short times or low temperatures). The creep properties are insensitive to age (time t_e) and they depend on the detailed chemical structure of the polymer. Specific molecular motions give rise to specific secondary retardation processes (*Figure 1*). For example, an n-alkyl side chain gives a secondary process with a retardation time of about 1 s at $-190°C$ (ref. 4). This process is only observed for $n \geqq 3$. In a material such as polyethylmethacrylate ($n = 2$) it is absent. Many other specific retardation processes are known and are comprehensively described in the literature[5,6].

Range II (longer times or higher temperatures). In this range, the behaviour is dramatically different. Some salient points include:

1. The creep curve strongly depends on age and it shifts to the right when t_e increases. An example is shown in *Figure 2*. Often, the ageing effects are very large, larger than the effects produced by a change in temperature of 40°C or more (cf. Figure 24 of ref. 1).
2. Creep curves measured at different temperatures can be superimposed by horizontal and vertical shifts in a double logarithmic ($\log J$ *versus* $\log t$) diagram (see *Figure 3*). This implies that the shape of the $\log J$ *versus* $\log t$ curve is independent of temperature (and age, point 1).
3. The shape of the $\log J$ *versus* $\log t$ curve hardly depends

* Now at: DSM Research, PO Box 18, 6160 MD Geleen, The Netherlands

0032-3861/89/050799-16$03.00

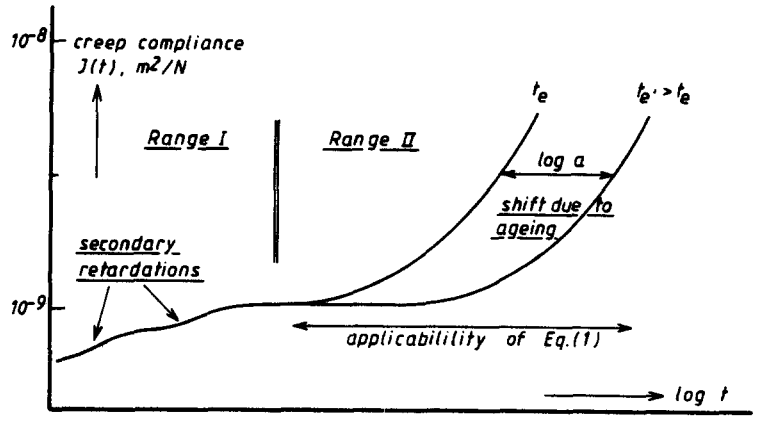

Figure 1 The general appearance of the creep curve of a glassy polymer measured at two times, t_e and t'_e, elapsed after quenching from above T_g to measuring temperature $T < T_g$. For details, see text

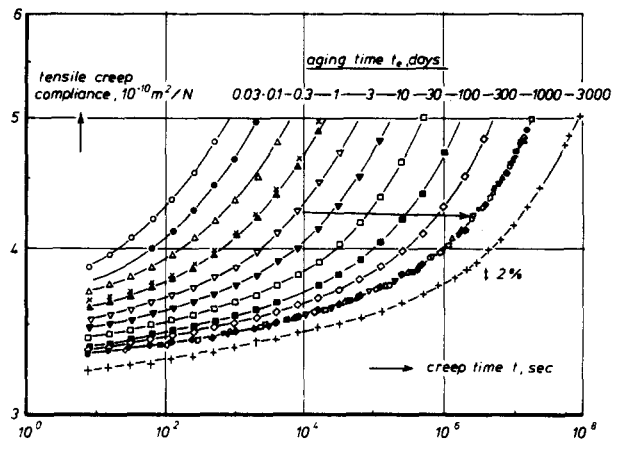

Figure 2 Small-strain tensile creep curves of rigid PVC quenched from 90°C (i.e. about 10°C above T_g) to 40°C and kept at 40±0.1°C for a period of 4 years. The different curves were measured for various values of the time t_e elapsed after the quench. The master curve gives the result of a superposition by shifts which were almost horizontal. The shifting direction is indicated by the arrow. The crosses refer to another sample quenched in the same way, but only measured for creep at a t_e of 1 day. Reproduced from reference 1 with permission

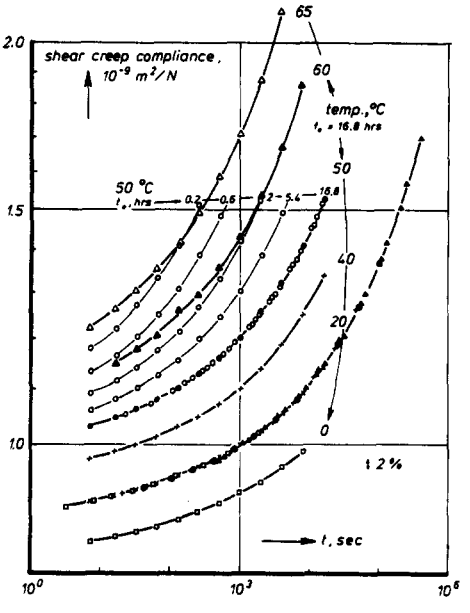

Figure 3 Small-strain torsional creep of rigid PVC quenched from 90°C to various temperatures. For 50°C, the curves are given for t_e equals 0.2, 0.6, 2, 5.4, and 16.8 h. These curves can be superimposed by almost horizontal shifts. The master curve is given by the circles and dots. The curves at different values of t_e for other temperatures are also superimposable, so we have only given the curves at a t_e of 16.8 h. By horizontal and vertical shifts, these curves at different temperatures can also be superimposed. The final master curve is given for a temperature of 20°C. The scatter around it is less than 1%. Reproduced from reference 1 with permission

on the specific chemical structure. It is the same for PS, PVC, SAN, etc. (cf. Figures 33 and 34 of ref. 1) and the creep can be described by the empirical formula:

$$J(t) = J_0 \, e^{(t/t_0)^\gamma} \qquad \gamma \sim 1/3 \qquad (1)$$

where $\log J_0$ and $\log t_0$ correspond to the vertical and horizontal shift factors in *Figures 2* and *3*. The constancy of γ expresses the fact that the shape of the creep curve ($\log J$ *versus* $\log t$) does not change with the chemical structure. It should be realized that equation (1) only holds for the onset of the glass–rubber transition. For temperatures at or above T_g, equation (1) is no longer valid (see later).

4. At temperatures sufficiently below T_g, the effect of temperature on creep is surprisingly small. Actually, parameter t_0 in equation (1) varies linearly with T and not with $\exp(H/RT)$ as is usual (Arrhenius behaviour). In fact, t_0 is proportional to $T_g - T$ and therefore the $\log a_T$ *versus* T curve flattens at low temperatures (see *Figure 4*, $\log a_T$ is the thermal shift $\log[t_0/(T_r)/t_0(T)]$ where T_r denotes some reference temperature and t_e is taken to be the same at all temperatures). The origin of this non-Arrhenius behaviour is discussed in Section 4.10 of reference 1.

5. Shift $\log a$ produced by isothermal ageing (see *Figure 1*) often varies linearly with $\log t_e$ (cf. Figure 25 of reference 1), which implies that the double-logarithmic shift rate μ remains constant:

$$\mu = d \log a / d \log t_e = \text{constant} \qquad (2)$$

This also implies that (see equation 1):

$$t_0(t_e) = t_0(t_{e_r})(t_e/t_{e_r})^\mu \qquad (3)$$

where t_{e_r} is some reference value of t_e.

6. The ageing kinetics hardly depends on the type of polymer. Shift rate μ is about unity for the temperature range of the type II behaviour. Usually, this range is bounded by T_g at the upper side and the temperature T_β

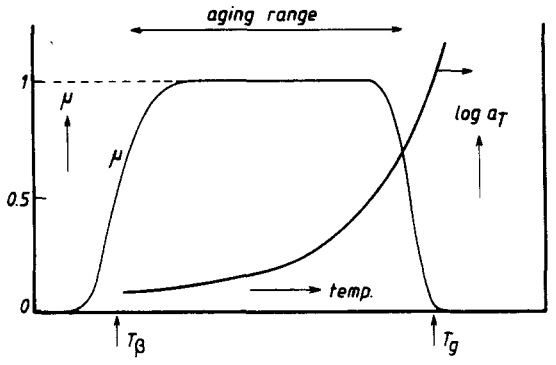

Figure 4 Effect of temperature T on ageing and creep of an amorphous polymer quenched from $T_0 > T_g$ to measuring temperature $T < T_g$. Shift rate μ is defined by equation (2). Log a_T is the (thermal) shift between creep curves measured at different temperatures but at a constant ageing time t_e. Log a_T is taken positive for an acceleration. T_β is defined in the text. Reproduced from reference 2 with permission

of the first secondary transition at the lower side (*Figure 4*). The typical difference with range I is that in range II there is little effect of chemical structure with a large effect of age.

METHODS TO PREDICT LONG TERM CREEP

We will now outline the long term creep theory developed in Chapters 10–12 of reference 1. For details refer to the original publication. To begin with, we have to distinguish between two types of tests yielding two types of properties. In a *short-time test* we keep testing time t short compared to the ageing time, t_e, at the beginning of the test (e.g. a 1 h test at a t_e of 100 h). The ageing during testing can be neglected (cf. equation (3)) and we obtain the so called momentary or short-time properties. Examples are the creep data shown in *Figures 2* and *3*. Momentary creep compliances are denoted by $J(t_e, t)$ (shear) or $F(t_e, t)$ (uniaxial extension). In a *long term test*, testing time t becomes much longer than the t_e at the beginning of the test. There is considerable ageing during testing and we obtain the so called long term properties. For creep, the long term compliances are denoted by $\bar{J}(t_e, t)$ or $\bar{F}(t_e, t)$. Note that the distinction between long and short term is not based on the absolute value of testing time t, but on the ratio t/t_e (e.g., a 1 year test at a t_e of 50 years yields the momentary properties).

There are large and fundamental differences between momentary and long term properties. For example, Boltzmann's superposition principle and the linear viscoelastic theory (which is based on that principle) do not apply to long term phenomena, even for infinitesimally small strains (the explicit time dependence of the properties due to ageing violates the superposition principle). By using the concept of effective times, the linear viscoelastic theory can, however, easily be generalized to ageing conditions. Further, most of the results mentioned in the previous section only apply to momentary properties. As will be seen later on, the long term compliance $\bar{J}(t_e, t)$ does not obey equation (1). Moreover, time–temperature superposition is impossible for $\bar{J}$.

An illustration of the differences between short and long term compliances is given in *Figure 5*. *Figure 5a* shows momentary creep curves ($t_e = 2$ h) at 20–70°C. As discussed previously, these curves can be superimposed; the resulting master curve is given for a temperature of 20°C. Similar master curves are given at 40–65°C by dashed lines. It is important to understand the proper meaning of these master curves. The one at 20°C was derived from short-time data (no simultaneous ageing) at 20–70°C. It seems logical to assume that this master curve gives the momentary creep compliance at 20°C and $t_e = 2$ h, i.e. the creep compliance that would be observed when, immediately after loading at $t_e = 2$ h, the ageing process had stopped and the creep would develop according to the properties at $t_e = 2$ h. This means, the master curve is a hypothetical creep curve. It can be determined unambiguously by time–temperature super-

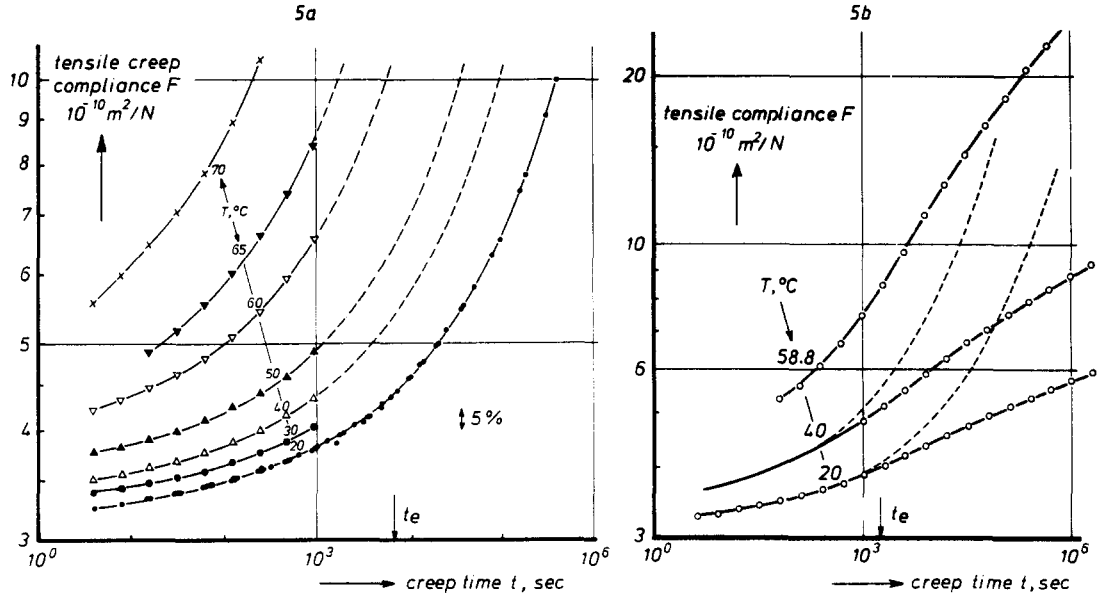

Figure 5 Small-strain tensile creep of rigid PVC. (a) Short-time tests ($t \leqq 1000$ s) at a t_e of 2 h after quenches from 90°C to various temperatures ($t/t_e < 0.14$). The master curve at 20°C was obtained by time–temperature superposition. The dashed curves indicate the master curves at other temperatures. (b) Long-term tests ($t \leqq 2.10^6$ s, $t_e = 0.5$ h, $t/t_e \leqq 1100$). The dashed lines are the master curves at 20 and 40°C for a t_e of 0.5 h. They were derived from the diagram in (a). Reproduced from reference 1 with permission

position of the data at 20–70°C but it cannot be measured at 20°C.

The master curves at 20 and 40°C are reproduced in *Figure 5b*, for a t_e of 0.5 h (dashed curves). These are compared with the actual long term creep curves (full lines) and we observe that the actual creep is much less than as predicted by the master curves. The reason will become clear: during the actual creep process, the material ages and continuously stiffens; therefore its creep will be less than expected from the momentary compliance. *Figure 5b* also clearly reveals the impossibility of time–temperature superposition for long term creep (the slope of the long term part of the curves increases with temperature) and the inapplicability of equation (1). (The curves are rather flat and show a small negative curvature at long times. Equation (1) predicts a positive curvature.)

In view of these results the first conclusion must be: the long term creep cannot be predicted by a simple time–temperature superposition of short-time data. Although the superposition technique works perfectly (*Figure 5a*), the resulting master curve gives the wrong information because the simultaneous ageing, which strongly affects long term creep, is not taken into account.

The simultaneous ageing effects can be described by the effective-time theory, originally developed for non-isothermal viscoelasticity[7,8]. This theory considers the case that the material properties are influenced by changes in temperature T only. Ageing effects are omitted for the moment. The basic assumption in the theory is that of thermo-rheological simplicity[9], i.e. the change in temperature only produces a shift of the creep curve along the logarithmic time scale without change in shape. In other words, all retardation processes contributing to the creep are accelerated (heating) or decelerated (cooling) by exactly the same factor. Let us take some temperature T_r as reference temperature. Let $a[T(t), T_r]$ be the acceleration factor and $J_r(t)$ the compliance at T_r (ageing effects are not taken into account here, see below). Time t is taken zero at the moment of loading (by stress σ_0). Consider now, at an arbitrary temperature course $T(t)$, the time interval between t and $t+dt$. During this interval *all* processes run $a(t)$ times faster than in the reference state at T_r. Consequently, the interval dt at temperature $T(t)$ is equivalent to an effective time interval $d\lambda$ at the reference temperature T_r:

$$d\lambda = a[T(t), T_r]\, dt \tag{4}$$

Similarly, the interval between $t=0$ and time t is equivalent to an effective time λ at T_r given by:

$$\lambda = \int_0^t a(\xi)\, d\xi \tag{5}$$

where ξ is an integration variable on the real t-time scale and where $a(\xi)$ denotes $a[T(\xi), T_r]$.

The word equivalent used previously means that the creep strain $\varepsilon(t)$ under non-isothermal conditions is given by:

$$\varepsilon(t) = \sigma_0 J_r[\lambda(t)] \tag{6}$$

So, if the temperature course $T(t)$ is known together with the acceleration function $a[T, T_r]$, the effective time λ can be calculated as a function of t (equation 5). Using equation (6), we can then express the non-isothermal creep in terms of the isothermal compliance at T_r.

This recipe can directly be applied to the long term creep problem, because ageing causes similar simple shifts along the logarithmic time scale (see *Figure 2*), as do changes in temperature for materials which behave thermorheologically simply. To elaborate this idea, we consider a creep test started at an elapsed time t_e. As reference state, we take the moment of loading (elapsed time t_e). So, J_r defined above is identical to the momentary compliance $J(t_e, t)$. The acceleration factor follows from equation (3). At creep time t, the elapsed (ageing) time has increased from t_e to t_e+t, so $a(t)$ is given by:

$$a(t) = \left(\frac{t_e}{t_e+t}\right)^{\mu} \tag{7}$$

Because ageing decelerates creep, $a(t)$ will be smaller than unity. Applying equation (5) we find:

$$\lambda(t) = t_e \ln[1+t/t_e] \tag{8}$$

if $\mu=1$ and

$$\lambda(t) = \frac{t_e}{\alpha}[(1+t/t_e)^{\alpha}-1] \tag{9}$$

if $0<\mu<1$ where:

$$0<\alpha=1-\mu<1 \tag{10}$$

Using equation (6) and writing $\bar{J}(t_e, t)$ for the long term compliance $\varepsilon(t)/\sigma_0$, we find:

$$\bar{J}(t_e, t) = J[t_e, \lambda(t)] \tag{11}$$

Thus, the prediction problem has been solved, i.e. we have found an expression of $\bar{J}$ in terms of momentary compliance J. The practical application is performed in three steps:

1. We determine the momentary compliance $J(t_e, t)$ at the temperature of interest by the time–temperature superposition method shown in *Figure 5a*.
2. Next, we determine shift rate μ from short-time tests at T for various values of ageing time t_e (cf. *Figure 2*); μ is found from the horizontal shifts of the creep curves by means of equation (2).
3. Finally, we calculate λ from t by means of equations (8) or (9) and determine the long-term compliance $\bar{J}(t_e, t)$ by means of equation (11).

Table 1 gives the λ–t relationships according to equations (8) and (9).

The above method is described in detail in Chapter 11 of reference 1. It has been checked by experiments on rigid PVC (see Figure 114 of reference 1) and it proved to yield reliable predictions for extrapolations of up to a factor of 100–1000 on the time scale.

On the basis of the theory given above, we could also derive a linear-extrapolation method. Such a method is already suggested by the data shown in *Figure 5b*: the long term creep curves are rather flat and extrapolations over 2–3 decades do not seem to lead to serious errors. The extrapolation errors were analysed theoretically as follows: we substituted the general formula (equation 1) for momentary creep into equation (11). It was found that the shape of the long term creep curve is determined by only two parameters, viz. the shift rate μ and the value of t_0 (see equation (1)) at ageing time t_e (start of creep test). Next, we varied these two parameters over the ranges which will be encountered in practice, and calculated the errors in linear extrapolations over 2 and 3 decades in a $\bar{J}$ *versus* $\log t$ (semi-log) and a $\log \bar{J}$ *versus* $\log t$ (double-log) diagram. The conclusion (Section

Table 1 Relation between real creep time t and effective creep time λ. The table, calculated using equations (8) and (9), gives λ/t_e for various values of μ

t/t_e	$\mu=$ 0.70	0.75	0.80	0.85	0.90	0.95	1.00
1	0.770	0.757	0.743	0.730	0.718	0.705	0.693
2	1.301	1.264	1.229	1.194	1.161	1.129	1.099
4	2.069	1.981	1.899	1.820	1.746	1.676	1.609
8	3.111	2.928	2.759	2.603	2.457	2.322	2.197
10	3.510	3.285	3.077	2.886	2.710	2.548	2.398
20	4.976	4.563	4.192	3.859	3.559	3.288	3.045
40	6.822	6.122	5.508	4.970	4.497	4.081	3.714
80	9.124	8.000	7.041	6.221	5.518	4.915	4.394
100	9.977	8.681	7.584	6.655	5.865	5.191	4.615
200	13.029	11.061	9.441	8.104	6.995	6.073	5.303
400	16.796	13.900	11.581	9.716	8.210	6.989	5.994
800	21.439	17.280	14.041	11.507	9.515	7.939	6.686
1000	23.152	18.499	14.909	12.125	9.955	8.252	6.909
2000	29.269	22.753	17.868	14.183	11.386	9.248	7.601
4000	36.802	27.813	21.267	16.466	12.920	10.279	8.294
8000	46.077	33.831	25.172	19.001	14.565	11.346	8.987
10000	49.498	36.001	26.548	19.874	15.119	11.698	9.210
20000	61.709	43.569	31.239	22.782	16.922	12.816	9.904
40000	76.742	52.569	36.628	26.009	18.854	13.973	10.597
80000	95.251	63.272	42.818	29.589	20.925	15.171	11.209

11.2 of ref. 1) was that the extrapolation can best be performed in a semi-log diagram and that the errors remain below 10–20% for extrapolation factors up to 1000. The conditions are that μ should be close to unity ($0.8<\mu<1$), that T should not be too close to T_g and that the creep time t, at which the extrapolation starts, is larger than t_e (it is only for $t>t_e$ that long term creep curves become more or less straight, see *Figure 5b*). Full details of the linear extrapolation method are given in Section 11.2 of ref. 1. A simple treatment, showing that the linearity of $\bar{J}$ *versus* $\log t$ is basically due to the ageing effects, is given in reference 10.

THE LONG TERM CREEP OF SEMI-CRYSTALLINE POLYMERS

We will now consider whether the methods described previously can be applied (or generalized) to semi-crystalline polymers. As stated in the introduction, we will treat the regions 1–4 one by one. The theoretical results will be compared with experimental data obtained on the materials described in reference 2. Details about the experimental techniques can be found in reference 1.

Region 1 $T<T_g^L$

Below T_g^L, the ageing and short-time creep behaviour of a semi-crystalline polymer is similar to that of an amorphous material[2]. We therefore expect that the prediction methods described earlier can be applied without modification.

This was verified by measurements on PET (37) (for material code numbers, see ref. 2). Some of the results are given in *Figures 6* and *7*. *Figure 6* pertains to the first prediction method of the previous section. From short-time tests at 40, 50 and 60°C (tests of 1024 s), we determined the master curve for the momentary compliance at a t_e of 0.5 h. Using the μ-value of 0.80, given in Figure 22 of ref. 2, we calculated the long term creep (crosses in *Figure 6*). Obviously, the agreement with the experimental long term creep curve (circles) is excellent.

The other prediction method described earlier was based on the fact that for creep times $t \gg t_e$, the long-term creep curves become almost straight. As seen in *Figures 6* and *7*, this also happens for PET, which demonstrates that the linear-extrapolation method can be applied without modification.

The data in *Figures 6* and *7* suggest that at very long creep times ($t \gg t_e$), the creep curves measured for different values of t_e tend to merge. For example, *Figure 7* suggests that the curves for $t_e=1$ and 24 h merge at $t=10^8$–10^9 s (3–30 years). This can be explained theoretically (see Figure 109 of ref. 1).

Region 2 $T \sim T_g^L$

In regions 2 and 3, the behaviour of semi-crystalline polymers is more complicated than that of amorphous glassy polymers (for details see ref. 2). The horizontal shifts due to ageing are now accompanied by substantial vertical shifts which are downwards in region 2 and upwards in region 3. Moreover, the short-time creep curves no longer obey equation (1) and, at least in region 3, time–temperature superposition of short-time creep data is no longer possible. Consequently, much of the basis upon which the methods of the previous section were developed has disappeared. We will now show, however, that, with minor modifications, both methods can still be applied to semi-crystalline polymers.

Theory. We start from the simplifying assumption made in ref. 2 that the (total) creep compliance $J(t_e, t)$ can be written as the sum of a contribution $J_1(t_e, t)$ of more mobile regions and a contribution $J_2(t_e, t)$ of the less mobile ones:

$$J(t_e, t)=J_1(t_e, t)+J_2(t_e, t) \tag{12}$$

Both contributions are affected by ageing in the usual way: they are shifted along the logarithmic time scale at shift rates μ_1 and μ_2, i.e.:

$$J_1(t_e, t)=J_1(t_{e_r}, (t_{e_r}/t_e)^{\mu_1}t) \tag{13}$$

$$J_2(t_e, t)=J_2(t_{e_r}, (t_{e_r}/t_e)^{\mu_2}t) \tag{14}$$

in which t_{e_r} is some reference value of t_e.

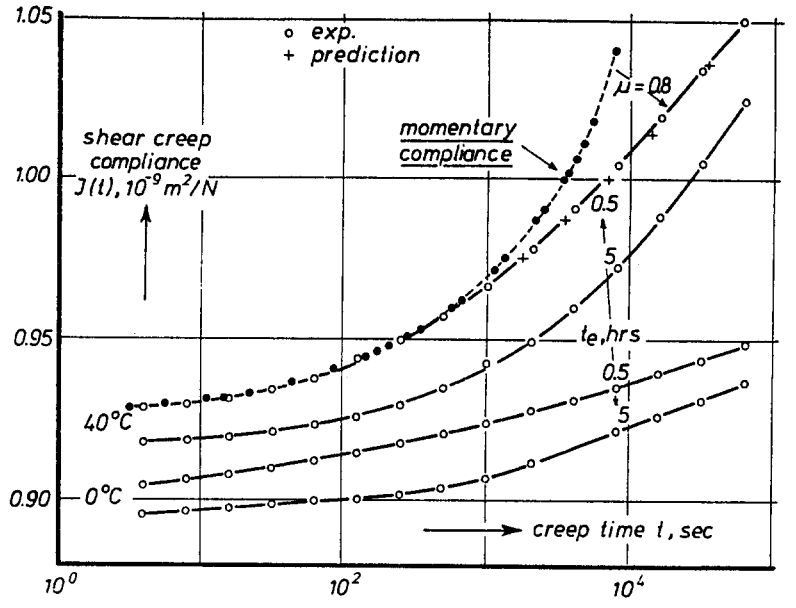

Figure 6 Long term small strain torsional creep (○) of semi-crystalline PET (37) at 0 and 40°C after quenches from 80°C. The momentary compliance at 40°C ($t_e = 0.5$ h) was obtained as described in the text; from this curve the long-term creep (+) was calculated using equations (8)–(11)

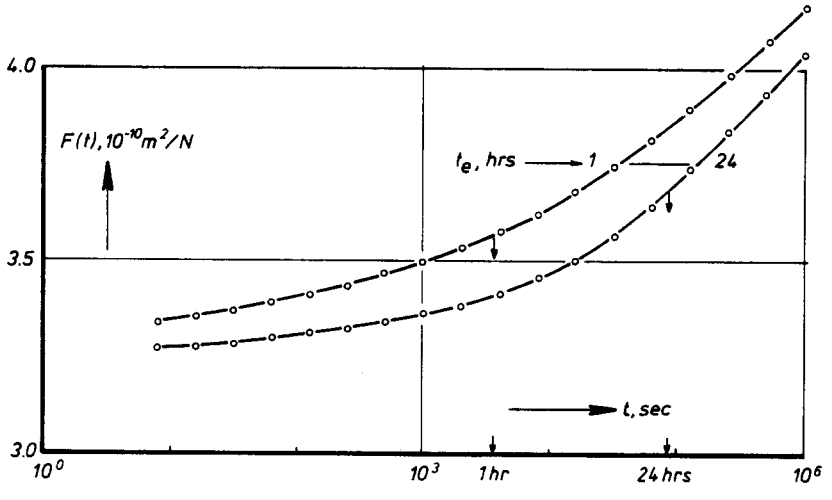

Figure 7 Long term tensile creep at small strains of PET (37), quenched from 120 to 20°C and tested after t_e of 1 and 24 h

Shift rates μ_1 and μ_2 are not equal; in region 2 we have[2]:

$$0 < \mu_1 < \mu_2 \sim 1 \tag{15}$$

Further, the time dependence of J_2 is much less than that of J_1. Actually, J_2 is only a correction term necessary to explain the (downward) vertical shifts (cf. Figure 6 of ref. 2).

Let us now elaborate the picture of Figure 6b of ref. 2. For abbreviation, we write

$$J_1(t_{e_r}, t) = \phi(t) \tag{16}$$

$$J_2(t_{e_r}, t) = A + C \ln t \tag{17}$$

in which A and C are constants.

Combining equations (12), (16) and (17) we obtain:

$$J(t_{e_r}, t) = \phi(t) + A + C \ln t \tag{18}$$

For $t_e > t_{e_r}$ we have: (cf. equations (13)–(14))

$$J_1(t_e, t) = \phi[(t_{e_r}/t_e)^{\mu_1} t] \tag{19}$$

$$J_2(t_e, t) = A + C \ln[(t_{e_r}/t_e)^{\mu_2} t] \tag{20}$$

Because of the logarithmic form of J_2 we can change equation (20) into:

$$J_2(t_e, t) = A + C \ln[(t_{e_r}/t_e)^{\mu_1} t] + C \ln[(t_{e_r}/t_e)^{\mu_2 - \mu_1}] \tag{21}$$

Equations (19) and (21) yield:

$$J(t_e, t) = \phi[(t_{e_r}/t_e)^{\mu_1} t] + A + C \ln[(t_{e_r}/t_e)^{\mu_1} t] + C(\mu_2 - \mu_1) \ln(t_{e_r}/t_e) \tag{22}$$

In view of equations (16)–(18), this is identical to:

$$J(t_e, t) = J(t_{e_r}, (t_{e_r}/t_e)^{\mu_1} t) - C(\mu_2 - \mu_1) \ln(t_e/t_{e_r}) \tag{23}$$

Equation (23) says that a change in age from t_{e_r} to $t_e > t_{e_r}$ causes two effects:

1. A horizontal shift of the total creep curve. The magnitude of the shift is determined by horizontal shift rate μ_1 and is given by $\mu_1 \ln(t_e/t_{e_r})$.
2. A downward vertical shift given by $C(\mu_2 - \mu_1) \ln(t_e/t_{e_r})$.

This is exactly the behaviour found experimentally[2] which justifies the treatment (equations 12–14). The vertical shift rate B defined by equation (7) of ref. 2 is found as:

$$B=-\frac{2.303(\mu_2-\mu_1)C}{J(t_e^*,t^*)} \tag{24}$$

Note that B is a relative shift rate (relative change in compliance per tenfold increase in t_e). It is for this reason that the vertical shift $2.303(\mu_2-\mu_1)C$ is divided by the compliance $J(t_e^*,t^*)$ at some arbitrarily chosen set of values of t_e and t. These values ($t_e^*=3$ h and $t^*=1024$ s) are given on page 1529 of ref. 2. Note further that factor $2.303=\ln(10)$ originates from the change from log to ln.

For the long term creep we now can proceed as follows. The assumption expressed by equation (12)–(14) 'saves' the effective time concept. This concept can be applied to J_1 and J_2 separately and we find:

$$\bar{J}(t_e,t)=\bar{J}_1(t_e,t)+\bar{J}_2(t_e,t) \tag{25}$$

where:

$$\bar{J}_1(t_e,t)=J_1[t_e,\lambda_1(t)] \tag{26}$$

$$\bar{J}_2(t_e,t)=J_2[t_e,\lambda_2(t)] \tag{27}$$

Reduced times λ_1 and λ_2 can be found from equations (8)–(10) by using the values μ_1 and μ_2 respectively.

Equations (25)–(27) yield:

$$\bar{J}(t_e,t)=J_1[t_e,\lambda_1(t)]+J_2[t_e,\lambda_2(t)] \tag{28}$$

We change this into:

$$\bar{J}(t_e,t)=J_1[t_e,\lambda_1(t)]+J_2[t_e,\lambda_1(t)]+\Psi \tag{29}$$

where:

$$\Psi=J_2[t_e,\lambda_2(t)]-J_2[t_e,\lambda_1(t)] \tag{30}$$

Instead of equation (29) we can write:

$$\bar{J}(t_e,t)=J[t_e,\lambda_1(t)]+\Psi \tag{31}$$

The first term in equation (31) is the long term compliance as calculated from the total momentary compliance (J_1+J_2) at ageing time t_e by using the shift rate μ_1 of J_1 only. According to equation (23), μ_1 follows from the horizontal component of the shift of the total creep compliance. The error introduced by the approximation is given by Ψ.

Error Ψ can be estimated as follows. Using equations (20) and (30) we find:

$$\Psi=J_2[t_e,\lambda_2(t)]-J_2[t_e,\lambda_1(t)]=C\ln(\lambda_2/\lambda_1) \tag{32}$$

Since $\mu_2>\mu_1$, λ_2 will be smaller than λ_1 (*Table 1*) and Ψ will be negative. Its absolute value $|\Psi|$ increases with increasing λ_1/λ_2 ratio, i.e. with increasing difference between μ_1 and μ_2 (see *Table 1*). To get the maximum error, we take $\mu_2=1$. Using equations (8)–(10) and (24) we then find for the relative error $R=|\Psi|/\bar{J}(t_e,t)$:

$$R=\frac{J(t_e^*,t^*)}{\bar{J}(t_e,t)}\frac{B}{2.303\alpha}\ln\left[\frac{\alpha\ln(1+t/t_e)}{(1+t/t_e)^\alpha-1}\right] \tag{33}$$

where $\alpha=1-\mu_1$.

The error according to equation (33) can easily be estimated. First, the t value in $\bar{J}(t_e,t)$ will be (much) greater than the t^* value (1024 s) in $J(t_e^*,t^*)$. Consequently, ratio $J(t_e^*,t^*)/\bar{J}(t_e,t)$ can be taken $\leqq 1$ provided that t_e is not much smaller than $t_e^*=3$ h. Evaluating the logarithmic function in equation (33), we then find that for $0<\alpha<1$ and $1<t/t_e<10^3$:

$$R\leqq 2B \tag{34}$$

According to Figures 19–25 of ref. 2, rate B in region 2 generally remains smaller than a few percent. Consequently, the error Ψ in equation (31) can safely be neglected, i.e.

$$\bar{J}(t_e,t)\cong J[t_e,\lambda_1(t)] \tag{35}$$

So, we can calculate the long term creep from the total momentary creep curve (i.e. the experimental (master) curve) and from the measured horizontal shift rate μ_1. In fact, this implies that the vertical shifts can be neglected in the calculation of $\bar{J}$, which means that the first difference between amorphous and semi-crystalline polymers (vertical shifts) does not affect the prediction method. To apply equation (35), we simply take the μ values of Figures 19–25 of ref. 2 (this μ value is in fact μ_1) and calculate λ_1 with equations (8)–(10) or with *Table 1*.

The next problem is to find the momentary compliance $J(t_e,\lambda)$ for time (λ_1) values much larger than t_e. As with amorphous polymers, $J(t_e,t)$ cannot be measured for $t\gg t_e$. Further, the time–temperature superposition method, used for amorphous polymers, cannot be used here. It is useless in region 3 and of only limited value in region 2[2]. So, we have to design some other technique.

The key to the solution of this problem is the fact that in regions 2 and 3, the creep will be dominated by those amorphous regions which are near their glass–rubber transition[2]. We therefore return to amorphous polymers and consider their creep behaviour at and just below T_g. An outline is given in *Figure 8*. At short times, we have the onset of the glass–rubber transition and for this part of the curve we can use equation (1). In the central part, equation (1) is invalid (dashed line). We have a region of constant double logarithmic slope, m_1, (cf. Figure 4 of ref. 2), and $J(t)$ can be described by the equation

$$J(t)=Dt^{m_1} \tag{36}$$

where D is a constant. This constant slope region is

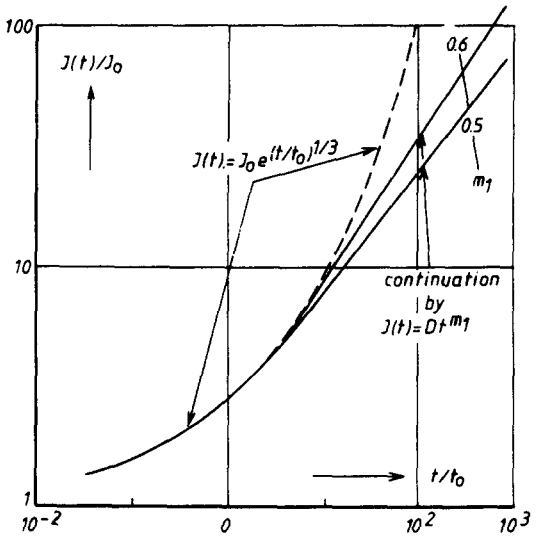

Figure 8 Creep of amorphous polymers in the onset and central part of the glass–rubber transition. J_0 denotes the glassy compliance (secondary relaxations are neglected, see *Figure 2*). The creep obeys empirical equation (1) at short times and empirical equation (36) in the central part. For details see text

several decades in time wide: it covers the region in which $J(t)$ increases to about 100 times the short time value (see Figure 4 of ref. 2). Slope m_1 is about 0.5. For the three polymers of Figure 4 of ref. 2 we have $m_1 = 0.57$ for PMMA, 0.53 for PUR and 0.58 for PVC.

In *Figure 8*, the creep is given for two values of slope m_1. The turnover from equation (1) to equation (36) is taken at the time, t_1, where the double log slope according to equation (1) equals m_1. Differentiation of equation (1) yields:

$$\mathrm{d}\ln J/\mathrm{d}\ln t = \gamma(t/t_0)^{\gamma} \qquad \gamma \sim 1/3 \tag{37}$$

So the turnover time t_1 is given by:

$$\gamma(t_1/t_0)^{\gamma} = m_1$$

or

$$t_1/t_0 = (m_1/\gamma)^{1/\gamma} \tag{38}$$

A plot of the semi-logarithmic creep rate $\mathrm{d}J/\mathrm{d}\ln t$, normalized by dividing by J_0 is given in *Figure 9*. The short-time part of the curve creep obeys equation (1), i.e.

$$\mathrm{d}J(t)/J_0/\mathrm{d}\ln t = \gamma(t/t_0)^{\gamma}\exp[(t/t_0)^{\gamma}] \qquad \gamma \sim 1/3 \tag{39}$$

The right half of the curves obeys equation (36), i.e.

$$\mathrm{d}J(t)/\mathrm{d}\ln t = m_1 D t^{m_1} \tag{40}$$

The two curves were matched (turnover point) as described before. This procedure leads to an artificial discontinuity in the slope of these curves, due to the arbitrary choice of the curve matching. As in *Figure 8*, the right half of the curves are given for two values of m_1.

Figure 9 shows that for amorphous polymers, the logarithm of the semi-logarithmic slope s, defined by

$$s = \mathrm{d}J(t)/\mathrm{d}\ln t \tag{41}$$

increases with $\ln t$ roughly in a linear way over the whole region of the onset and central part of the glass transition. This is shown in *Figure 9* for the case of $m_1 = 0.5$. The dashed straight line matches the full curve to within 20% over the whole time range ($10^{-2} < t/t_0 < 10^{+2}$).

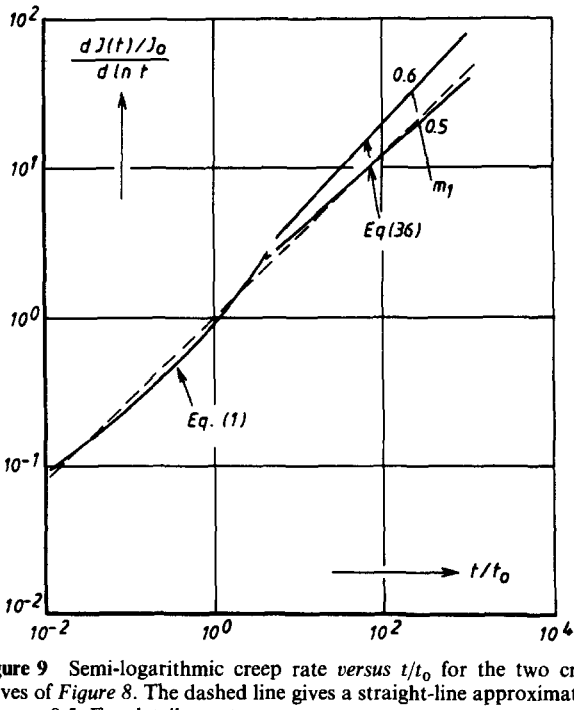

Figure 9 Semi-logarithmic creep rate *versus* t/t_0 for the two creep curves of *Figure 8*. The dashed line gives a straight-line approximation for $m_1 = 0.5$. For details see text

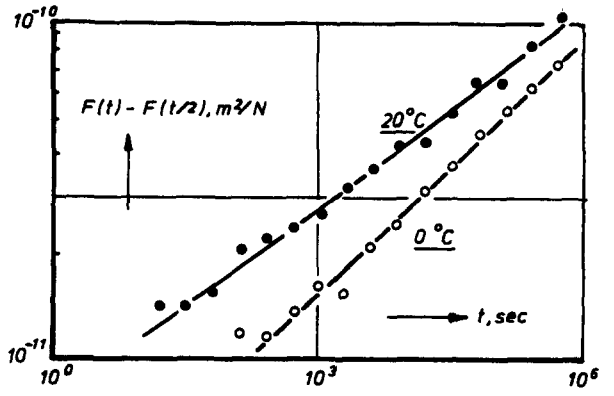

Figure 10 Semi-logarithmic slope (tensile creep), expressed as $F(t) - F(t/2)$, for PP (43) quenched from 120 to 0 and 20°C, and tested after elapsed time t_e of 10 days (8.64×10^5 s). The data are derived from those given in Figure 17 of reference 2

As can easily be verified, the approximate linearity of $\ln s$ with $\ln t$ implies that $J(t)$ can be written as:

$$J(t) \sim c + kt^m \tag{42}$$

in which c and k are constants. Instead of equations (1) and (36), equation (42) is applicable over the whole range (onset plus central part).

Let us now apply these results to the semi-crystalline polymers in region 2. The creep is dominated by that of the amorphous regions which are close to their glass transition. So, we expect that slope s will vary linearly with t in a log–log plot. Because for semi-crystalline polymers the glass transition is more smeared-out than in amorphous polymers, we also expect that the slope, m, will be smaller than in *Figure 9*. This is exactly the behaviour that has been found. An example for PP is given in *Figure 10* in which the semi-log slope is given as $F(t) - F(t/2) \sim \ln 2 \times \mathrm{d}F/\mathrm{d}\ln t$. More data on PP and HDPE are given in *Figure 11*.

These results suggest that we can find the momentary compliance $J(t_e, t)$ for $t \gg t_e$ by extrapolation of plots such as given in *Figures 10* and *11*. This in fact implies that we extrapolate according to equation (42) whilst the constants c, k, and m are determined from the $J(t_e, t)$ data for $t < t_e$.

Predictions based on the calculation of effective times. We will now apply the theory of the previous section to predict the long term creep of semi-crystalline polymers in region 2. For illustration, we will use the data on PP given in *Figure 12*.

The prediction method comprises four steps:

1. Shift rates μ and B are determined from short-time ageing tests. For PP (43) at 20°C, we obtain $\mu = 0.70$ and $B = -3\%$/decade (cf. the data on a slightly different PP in Figures 11 and 21 of ref. 2.) The pertinent t_e values varied from 0.35–6 h.
2. The short-time part of momentary compliance $F(t_e, t)$ is measured directly. In *Figure 12*, it is given ($t_e = 0.82$) by the open circles and the heavy curve. The data points at 512–2048 s (t comparable with t_e) were corrected as described on page 140 of ref. 1.
3. The long time part of $F(t_e, t)$ (i.e. for $t \gg t_e$) is found by plotting $F(t) - F(t/2)$ *versus* t in a double-log diagram. For PP (43), the data are given in *Figure 11* and in the insert of *Figure 12*. The dashed line (*Figure 11*) is the

extrapolation, it is given in *Figure 12* by the full curve.

4. The long-term compliance $\bar{F}(t_e, t)$ is determined by means of equation (35). The λ-values are found from equations (8)–(10) with the μ-value found under point (1). As shown in *Figure 12*, the prediction agrees perfectly with experiment.

Figure 12 also shows the creep at $t_e = 50$ h, which was predicted as follows. From the μ and B values given in the caption to *Figure 12*, we know how to shift the momentary compliance $F(t_e, t)$ when t_e is taken to be 50 instead of 0.82 h. Performing this shift, we obtain $F(t_e, t)$ at 50 h (full curve), and applying equations (8)–(10) we can again calculate the long term creep. (Note that the B value is only used to shift the momentary creep curve from $t_e = 0.82$ to its position at $t_e = 50$ h; the B value is not used in the calculation of $\bar{F}$ from F). Similar results are given in *Figures 13, 14* and *15*. In *Figure 13*, we have indicated the maximum variations in the prediction which result when the lines in *Figure 11* are drawn through the points at 40°C in different ways. The variations are clearly smaller than a few percent.

Figures 12–15 show that the prediction method works satisfactorily in all cases. Even for extrapolation factors of about 1000, the errors are less than a few percent.

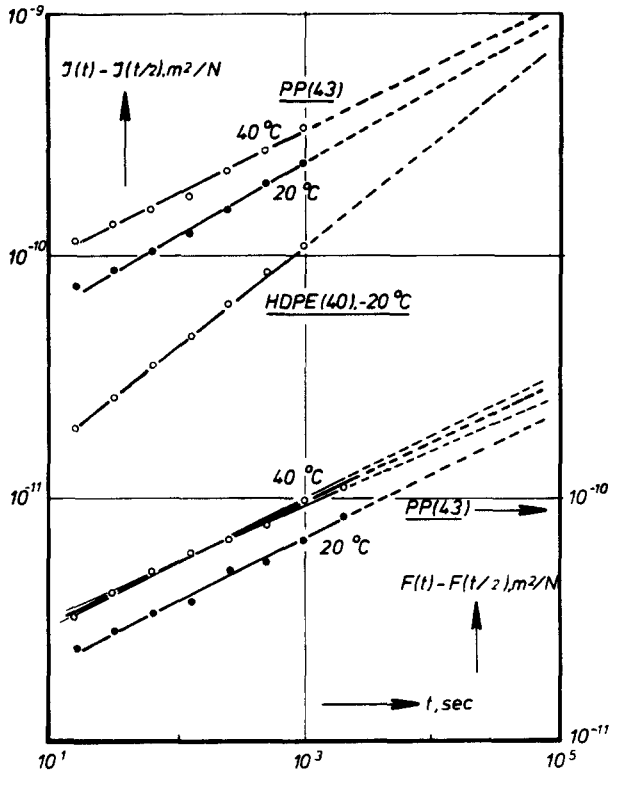

Figure 11 $J(t) - J(t/2)$ or $F(t) - F(t/2)$ *versus* time t for the tests dealt with in *Figures 12–14*. For details see text

Linear-extrapolation method. Figures 12–15 reveal that the long term creep curves are more or less straight for $t \gg t_e$. This suggests that the linear extrapolation method, developed for amorphous polymers[1], can be applied without modification. To find the extrapolation errors, we used the same technique as in Section 11.2 of ref. 1, now, however, on the basis of equation (42). Using equations (8)–(10), we find:

$$J(t) = c + kt^m \tag{43}$$

$$\bar{J}(t) = c + kt_e^m \ln^m(1 + t/t_e) \tag{44}$$

if $\mu = 1$

$$\bar{J}(t) = c + k(t_e/\alpha)^m[(1 + t/t_e)^\alpha - 1]^m \tag{45}$$

if $\mu < 1$

$$\alpha = 1 - \mu \tag{46}$$

For simplicity, we write $J(t)$ instead of $J(t_e, t)$.

We now consider the linear extrapolation

$$\bar{J}^*(t) = \bar{J}(t_1) + (\mathrm{d}\bar{J}/\mathrm{d} \ln t)_{t_1} \ln(t/t_1) \tag{47}$$

where $t > t_1$; t_1 is the maximum testing (creep) time and

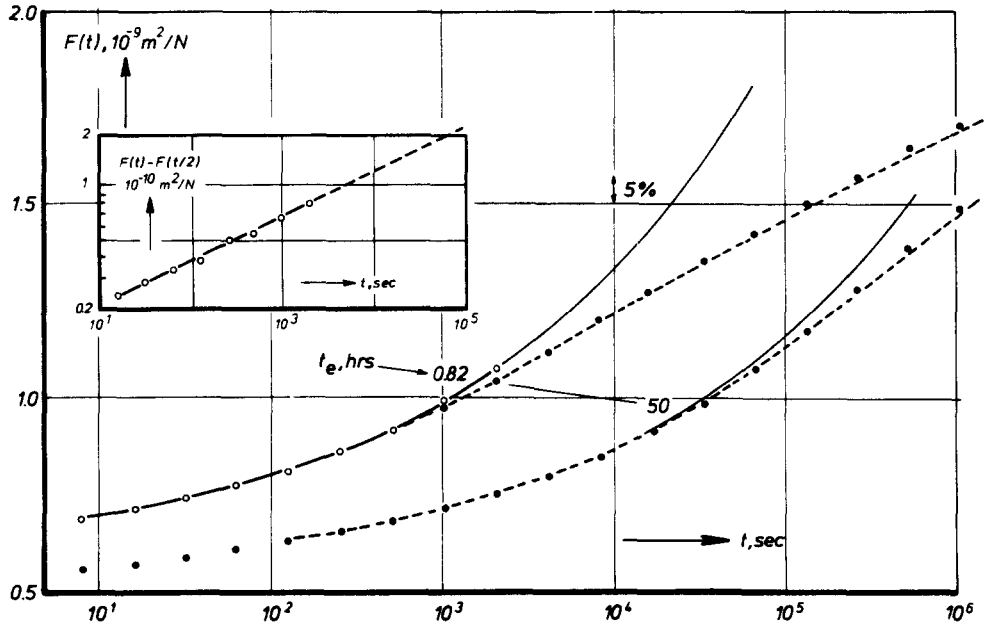

Figure 12 Small-strain tensile creep of PP (43) at 0.82 and 50 h after a quench from 120 to 20°C. For explanation, see text. —○—, momentary creep curve; – – – – –, long-term creep predicted from the momentary creep curve using $\mu = 0.70$; ●, actual long-term creep. The insert reproduces the pertinent data (PP, 20°C, tensile creep) from *Figure 11*

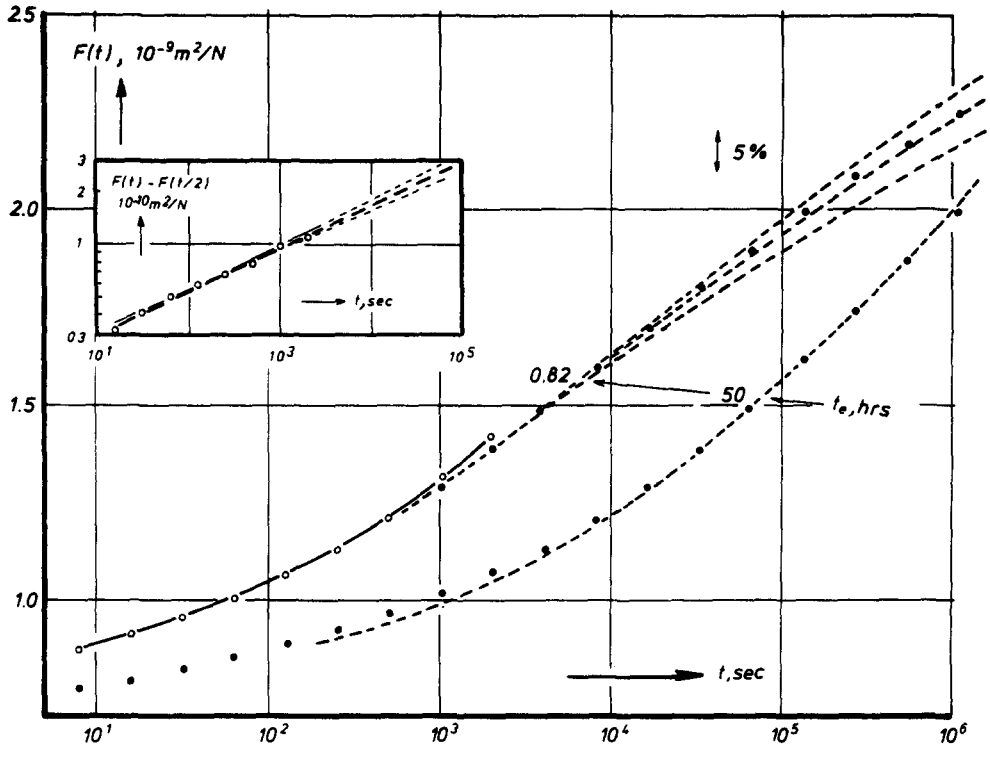

Figure 13 As *Figure 12*, but for $T=40°C$ ($\mu=0.70$, $B=0$). The pertinent data from *Figure 11* are reproduced in the insert

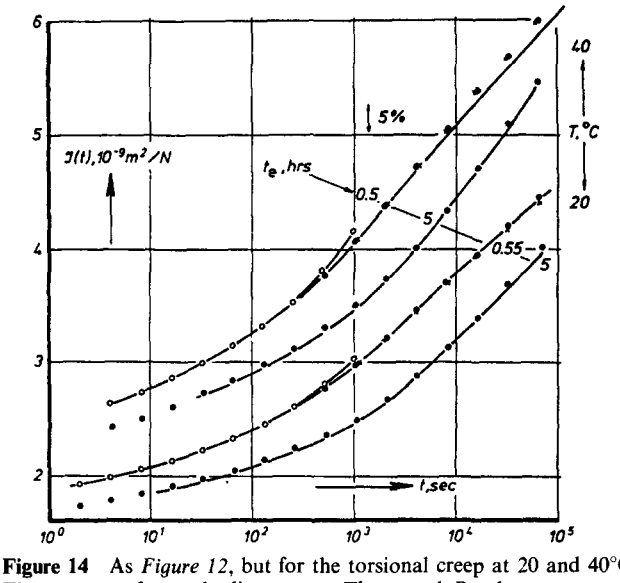

Figure 14 As *Figure 12*, but for the torsional creep at 20 and 40°C. The crosses refer to duplicate tests. The μ and B values were as in *Figures 12* and *13* (for the use of B see text). The momentary creep curves (—○—) were obtained using the data from *Figure 11* (torsional creep, PP, 20 and 40°C)

$t/t_1 = a$ = extrapolation factor. This extrapolation factor a should not be confused with acceleration factor a.

So, we find $\bar{J}(t)$ from $\bar{J}(t_1)$ by a linear extrapolation according to the slope at t_1 (slope on log time scale).

The relative extrapolation error q is given by

$$q=\frac{\bar{J}^*(t)-\bar{J}(t)}{\bar{J}(t)}=\frac{\bar{J}^*(t)-\bar{J}(t)}{\bar{J}(t)-c}\times\frac{\bar{J}(t)-c}{\bar{J}(t)}=r\frac{\bar{J}(t)-c}{\bar{J}(t)} \quad (48)$$

in which r is defined by

$$Q=1+r=\frac{\bar{J}^*(t)-c}{\bar{J}(t)-c} \quad (49)$$

According to equations (44) and (45), we have: $\bar{J}(t)>c$. Therefore equation (48) shows that $q<r$. So, to find the maximum errors, we only have to consider quantity $r=Q-1$. Substitution of equations (44) and (45) in (49) yields:

$$Q=\left\{\frac{\ln(1+x)}{\ln(1+ax)}\right\}^m\left\{1+\frac{m\ln a}{\ln(1+x)}\frac{x}{1+x}\right\} \quad \text{if } \mu=1 \quad (50)$$

$$Q=\left\{\frac{(1+x)^\alpha-1}{(1+ax)^\alpha-1}\right\}^m\left\{1+\frac{\alpha m\ln a}{1-(1+x)^{-\alpha}}\frac{x}{1+x}\right\} \quad \mu<1 \quad (51)$$

where

$$x=t_1/t_e \qquad \alpha=1-\mu \qquad Q=1+r \quad (52)$$

Figures 16 and *17* give $r=Q-1$ as a function of $x=t_1/t_e$ for various values of μ (0.6–1.0) and m (0.2, 0.3 and 0.4). The extrapolation factor a is 100 in *Figure 16* and 1000 in *Figure 17*. The figures show that the errors strongly depend on the parameters μ and m. They increase (or become less negative) with increasing value of μ; for $\mu=1$ the errors are always positive. For $m=0$, the errors are zero (see equations (50)–(51)) and with increasing m, the dependence on μ increases. Generally, the errors are the smallest for $\mu\sim0.8$.

For a number of semi-crystalline polymers (HDPE, LDPE, PP, PET, Nylon 6 and 12) the μ and m values can be obtained from Figures 19–24 of ref. 2. We observe that, in region 2, the μ value varies between 0.6 and 0.8 in most cases; only for HDPE, μ falls to 0.5 (Figure 19 of ref. 2). The m values can be derived from the $\tan\delta$ curves of Figures 19–24 of ref. 2, because $\tan\delta$ was calculated from the creep rate (equation (5) of ref. 2):

$$\tan\delta=\frac{\pi}{2}\,\mathrm{d}\ln J/\mathrm{d}\ln t \quad (52)$$

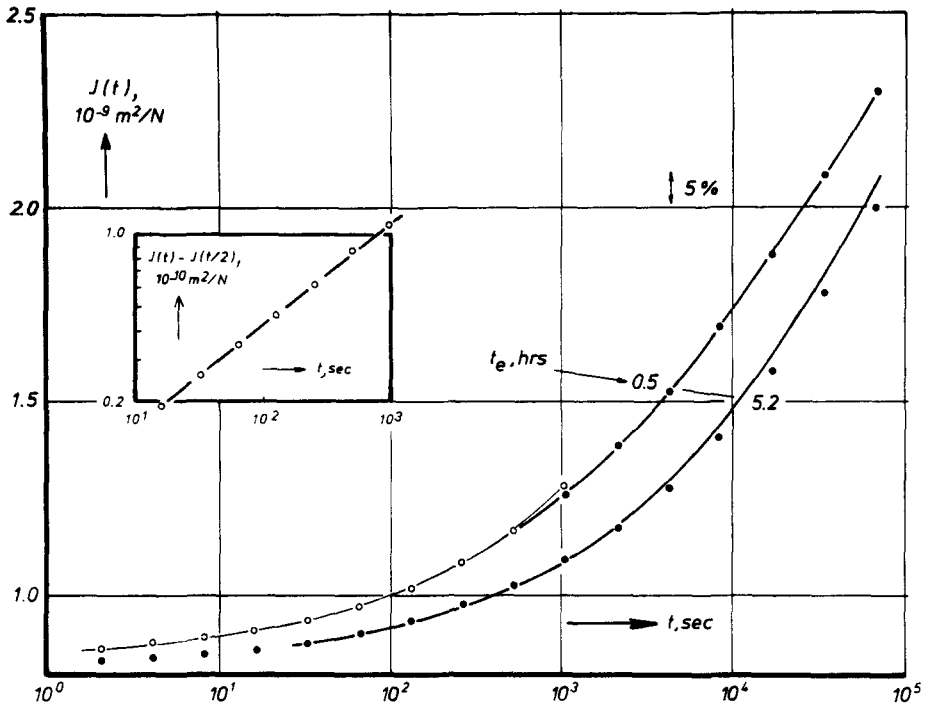

Figure 15 As *Figure 12*, but for HDPE (40) quenched from 100 to −20°C, and measured in torsion. According to Figure 19 of reference 2, we took $\mu=0.52$ and $B=-2\%$/decade (for the use of B see text). The insert reproduces the HDPE data from *Figure 11*

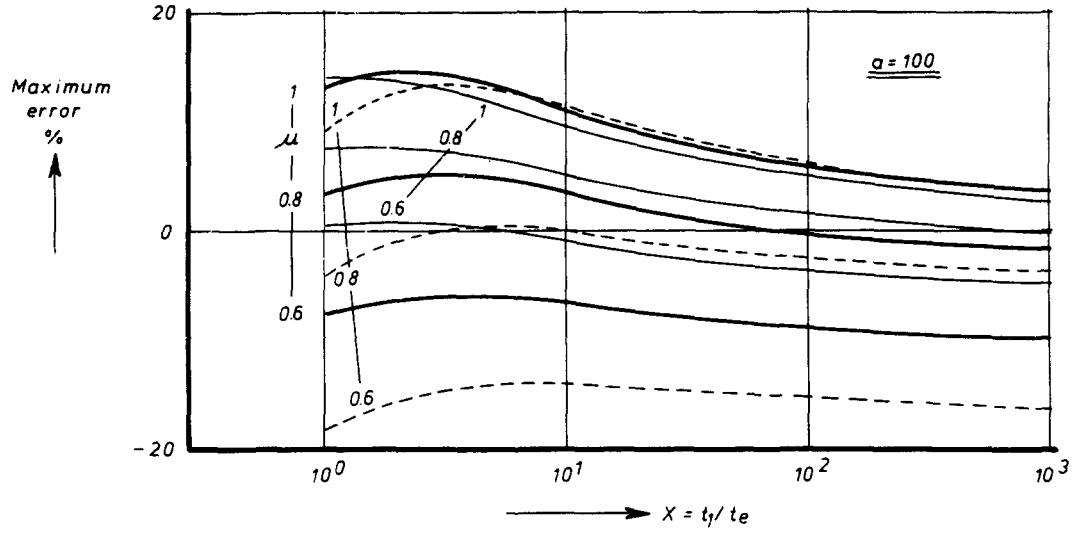

Figure 16 Maximum extrapolation error r according to equations (50)–(52) as a function of $x=t_1/t_e$ for various values of μ and m; $a=100$. ——, $m=0.2$; ———, $m=0.3$; – – –, $m=0.4$

Using equation (43), we thus find:

$$m \leqq \frac{2}{\pi} \tan \delta$$

Note that parameter m defined by equation (43) has a slightly different meaning from the one in ref. 2.

Inspection of Figures 19–24 of ref. 2 shows that $\tan \delta < 0.25$. Consequently, $m < 0.2$. These results imply that the data for $m=0.2$ in *Figures 16* and *17* (thin curves) give bounds for the extrapolation errors in most cases. Taking $t_1/t_e=1$, we obtain (maximum) errors between 0 and 7.5% for $a=100$ and between -1 and $+14\%$ for $a=1000$.This explains why the linear extrapolation method works reasonably well for semi-crystalline polymers.

Generally, the errors will be positive, i.e. the $\bar{F}$ (or $\bar{J}$) *versus* log t curves will show a slightly decreasing slope (cf. *Figures 12, 13* and *14*). Interestingly, theory (*Figures 16, 17*) predicts a negative error (upward curvature in $\bar{F}$ (or $\bar{J}$) *versus* log t) for $\mu=0.5$. Such a low μ value applies to HDPE at −20°C (see Figure 20 of ref. 2), and indeed, the long-term creep of HDPE at −20°C shows a slight upward curvature (*Figure 15*).

Region 3 $T_g^L < T < T_g^U$

We will now show that the methods described in the last section can also be used for region 3. As shown in ref. 2, the creep in this region can be written as:

$$J(t_e, t) = J_1(t) + J_2(t_e, t) \qquad (53)$$

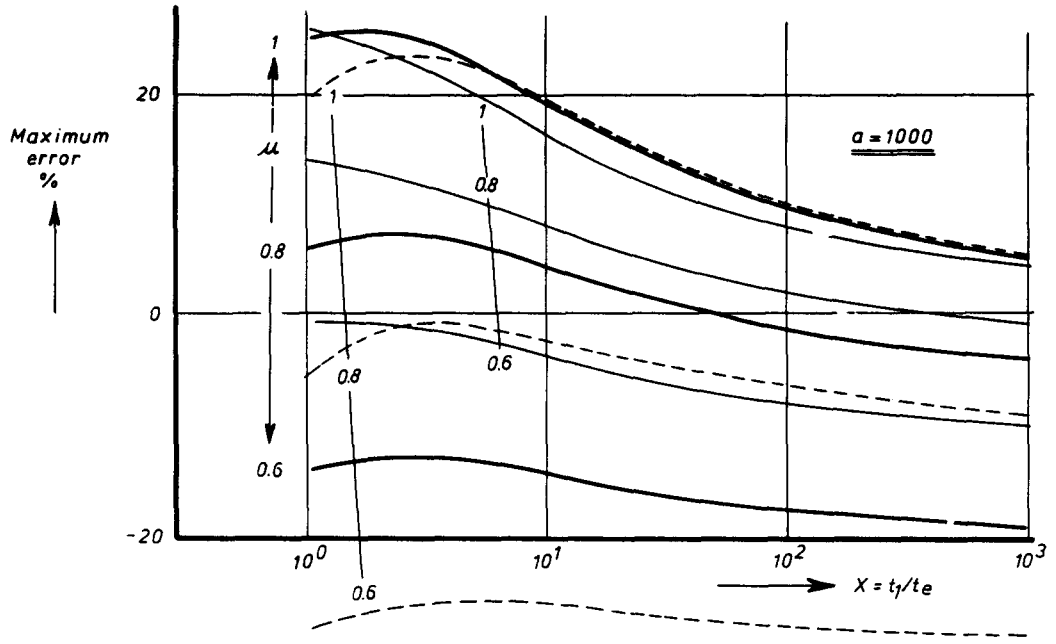

Figure 17 As *Figure 16*, but for $a=1000$

Creep component J_1 refers to the more mobile regions. These are above their T_g and no longer sensitive to ageing. J_2 refers to the less mobile regions which are at or just below their T_g.

Comparison with equations (12)–(14) shows that equation (53) is a special case of equation (12), namely with $\mu_1=0$. Further, if $J_1(t)$ can be written as (cf. Figure 7 of ref. 2):

$$J_1(t)=A'+C'\ln t \tag{54}$$

in which A' and C' are independent of t_e, the formalism reduces that of the theory section. It can easily be deduced that ageing produces horizontal shifts of the creep curve to the right (shift $=\mu_2\ln(t_e/t_{e_r})$),combined with upward vertical shifts of magnitude $\mu_2 C'\ln(t_e/t_{e_r})$. The vertical shift rate B defined in reference 2 is again given by equation (24), but now with the minus sign replaced by a plus sign, $\mu_2>\mu_1=0$ and C' instead of C.

The long term creep can again be calculated by means of equation (35) but now with λ_2 instead of λ_1. The errors are negative. Using equation (35) we consider creep component J_1 as being sensitive to ageing. This is incorrect (see equation (53)). Therefore the predicted value of $\bar{J}$ will be too low. The error Ψ is found by interchanging λ_1 and λ_2 in equation (32); because $\lambda_1=t$ ($\mu_1=0$) we obtain:

$$\Psi=C'\ln(t/\lambda_2) \tag{55}$$

Because $\lambda_2\leqq t$ (see *Table 1*), Ψ will be positive.

The errors are the largest for $\mu_2=1$. In that case the relative errors are given by equation (33) with $\alpha=1$ ($\mu_1=0$). Consequently, (we again use $J(t_e^*,t^*)\leqq\bar{J}(t_e,t)$, see earlier discussion):

$$R\leqq\left|\frac{B}{2.303}\ln\left(\frac{\ln(1+t/t_e)}{t/t_e}\right)\right| \tag{56}$$

For $t/t_e=10$, 100 and 1000 the errors are respectively $-0.63B$, $-1.34B$ and $-2.16B$. Consequently, as long as B is small compared to unity, the errors can be neglected, i.e. we can use the same methods as for region 2.

Inspection of Figures 19–24 of ref. 2 shows that B increases to 0.15 for the highest temperatures in region 3. Thus at these temperatures the errors may become large (20% for $t/t_e=100$).

Some experimental results are shown in *Figures 18* and *19*. *Figure 18* deals with HDPE, quenched to 20°C and measured at a t_e of 1 h. The short-time creep curve (2–1024 s) is given by open circles. From these data we calculated $F(t)-F(t/2)$ as a function of time. The results are given in the insert in *Figure 18*. By extrapolating the straight line, we found the momentary compliance (thin curve) and from this, we finally calculated the long term creep. The value of μ was taken from Figure 19 of ref. 2.

The curve drawn in Figure 19 of ref. 2 gives $\mu=0.65$, but, in view of the scatter and the strong temperature dependence of μ, values of 0.75–0.80 are also possible. All these values yield good predictions of the long term creep. Even for an extrapolation factor of 1000, the errors are less than about 10% (*Figure 18*).

Similar results for temperatures other than 20°C are given in *Figure 19*. There the long term creep has been calculated with μ values of 0.65 at 20°C, 0.75 at 30°C, 0.9 at 40°C, and 1 at 50, 60 and 70°C (cf. Figure 19 of ref. 2). At all temperatures, the extrapolation factor equals 100, and the errors are less than 5%.

Figure 19 also shows that in region 3, the (long term) creep curves measured at different temperatures cannot be superimposed. The double logarithmic slope of the creep curves decreases with increasing temperature. This inapplicability of time–temperature superposition is quite normal for long term creep. Also the short-time creep curves cannot be superimposed. This is a typical feature of region 3 as was discussed in ref. 2.

Region 4 $T\geqq T_g^U$

In this region, the ageing effects characteristic of regions 1–3, have disappeared. If there are no crystallization processes, the material will behave as a normal polymer above its T_g. There are no ageing effects, and no differences between momentary and long term com-

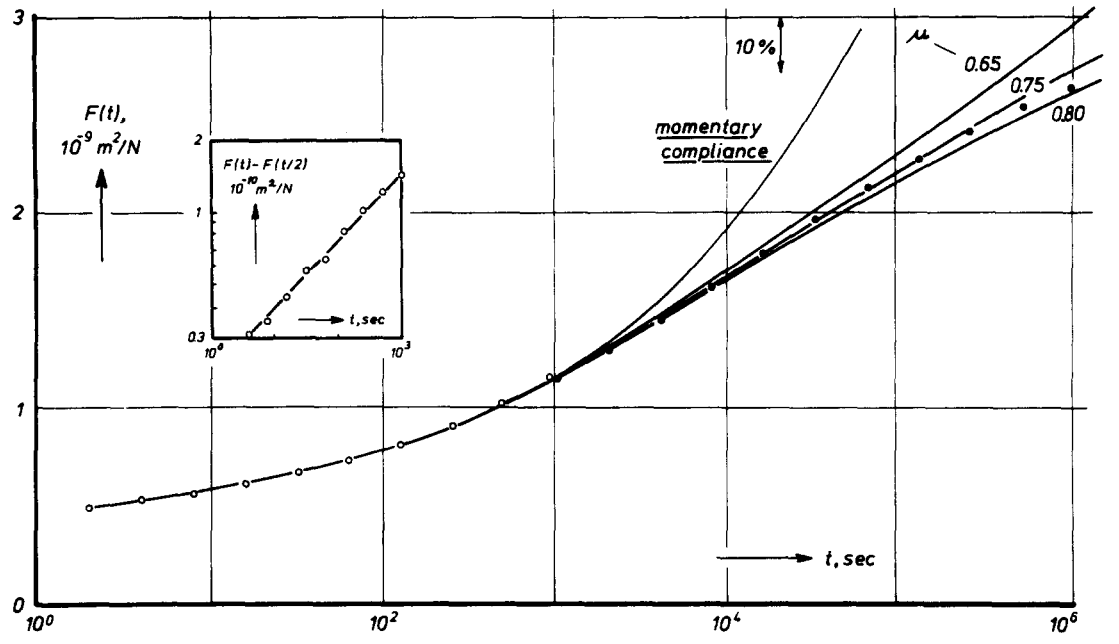

Figure 18 Small-strain tensile creep of HDPE (40) at 1 h after a quench from 80 to 20°C. ——○——, short time creep curve (points at 512 and 1024 corrected according to page 140 of reference 1); ——, predicted long term creep for various values of μ; ●, actual long term creep. The insert gives a plot similar to those of *Figure 11*

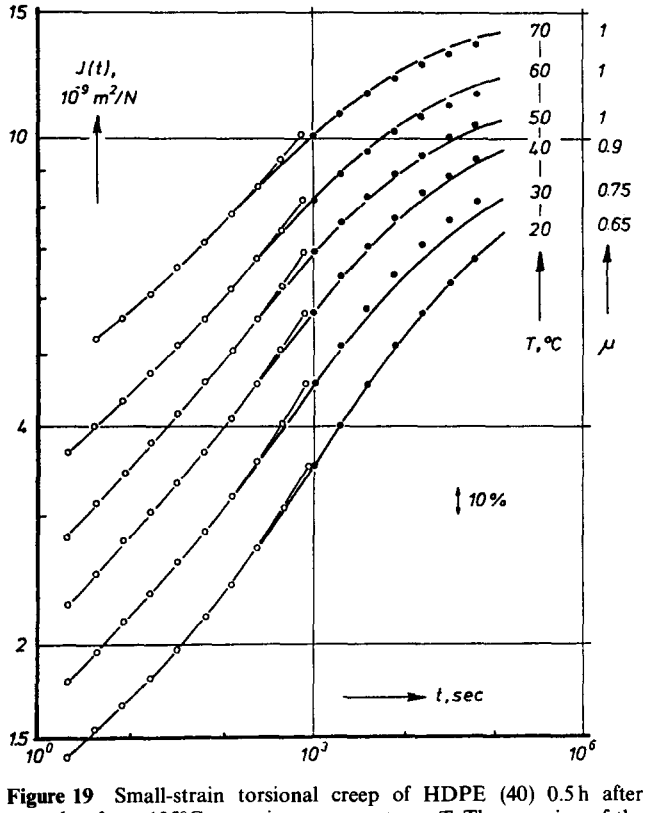

Figure 19 Small-strain torsional creep of HDPE (40) 0.5 h after quenches from 105°C to various temperatures T. The meaning of the symbols and curves is the same as in *Figure 18*. Note that the diagram is double-logarithmic

pliances. Furthermore, the creep curves measured at different temperatures can be superimposed by shifting in a double-logarithmic diagram. This means that the long term creep can be predicted by time–temperature superposition of short-time data.

Experimental data supporting this conclusion are shown in *Figure 20*. The short-time tests (torsional creep) lasted 1024 s. The master curves at 20 and 50°C were obtained by time–temperature superposition (horizontal and vertical shifts in a $\log J$ *versus* $\log t$ diagram; the arrow denotes the shifting direction). The experimental long term creep is indicated by crosses; the extrapolation factor a is 100. Obviously, experiment and prediction agree reasonably well.

Some other data on LDPE are shown in *Figure 21*. The curves are the master curves of *Figure 20*, but now for t_e values of 1 and 24 h. The torsion data (shear) were converted to tensile compliances by multiplying J by a factor of 1/3 (LDPE is very soft at 20°C; Poisson ratio is close to 0.5). *Figure 21* also shows experimental long term creep (crosses). The agreement is again good. (Note that the extrapolation factor is 1000 in *Figure 21*). In view of these results, we conclude that for region 4, the long term creep can indeed be obtained by time–temperature superposition.

In the preceeding discussion on LDPE, we tacitly disregarded the fact that LDPE is not insensitive to ageing at 20–70°C. As shown in Figure 13 of ref. 2, an increase in t_e effects a downward vertical shift of the creep curve (at 40°C about −10%/decade). The horizontal shifts, however, are small. The same results have been reported earlier (see, for example, ref. 11). In ref. 2, we suggested that this effect can be explained from secondary crystallization (see *Figure 8* and page 1532 of ref. 2).

We will now give a tentative explanation for the fact that such crystallization effects (downward shifts) do not disturb the prediction method. We start from the very crude model depicted in *Figure 22*. Suppose that the creep is due to interlamellar shear[12] of the soft amorphous layer which has a compliance $\phi(t)$. Assume further that the layer thickness l slowly decreases with the time t_e after quenching, but that the creep compliance $\phi(t)$ of the amorphous layer is insensitive to t_e. Assume finally that l decreases linearly with $\ln t_e$ (this is suggested by e.g. the volume relaxation data of Kovacs[13], obtained on LDPE as well as by Figure 15 of ref. 2).

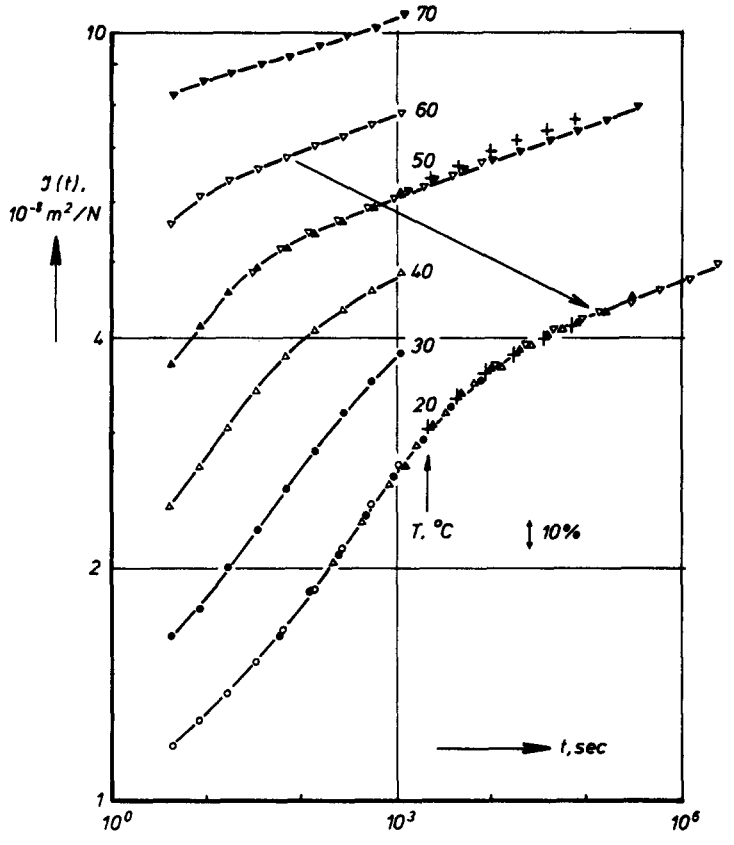

Figure 20 Small-strain torsional creep of LDPE (41) 0.5 h after quenches from 95°C to various temperatures, T. For details, see text

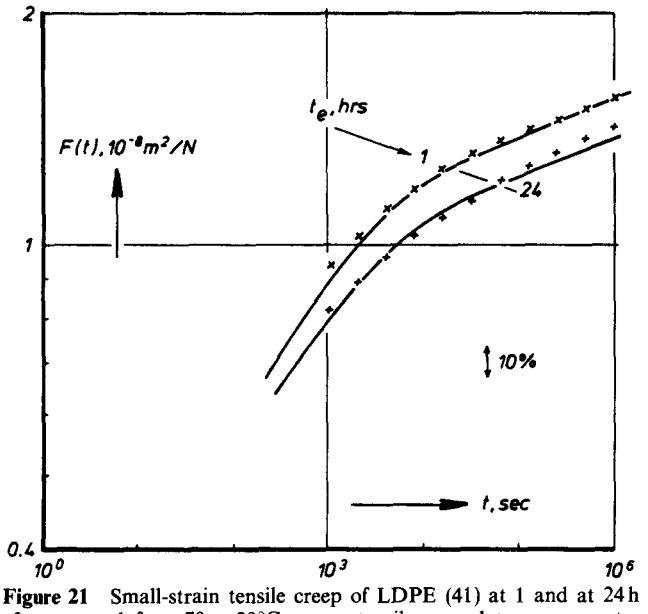

Figure 21 Small-strain tensile creep of LDPE (41) at 1 and at 24 h after a quench from 70 to 20°C. +, ×, tensile creep data; ——, master curve of *Figure 20* (but now at values of t_e of 1 and 24 h), converted to tensile compliances by assuming a Poisson ratio of 0.5

Short-time tests. As long as creep time $t \ll t_e$, the changes in l during testing can be neglected. This implies that the short time compliance $J(t)$ is proportional to $l(t_e)\phi(t)$. Thus, the changes in l can be found from the changes in the isochronous values of $J(t)$ with t_e. For $\mu = 0$, vertical shift rate B defined in ref. 2 becomes:

$$B = \frac{1}{J(t)} \frac{dJ(t)}{d \log t_e} \tag{57}$$

Consequently, a rate of $-100B\%$/decade implies that

$$l = l_0 \left(1 - \frac{B}{2.303} \ln t_e \right) \tag{58}$$

where l_0 is the l value at $t_e = 1$ h, whilst t_e is expressed in hours.

Long term creep. In this case l changes during creep. We assume that the transformation of amorphous to crystalline material does not produce a change in strain. We consider the small time interval between t and $t' = \Delta t + t$. Between t and t', the thickness of the amorphous layer decreases from l and $l' < l$. Due to the assumption made above, this decrease in thickness does not produce any change in strain. So, the change in strain γ is entirely due to the continued creep of the remaining amorphous layer:

$$\gamma(t') - \gamma(t) = \sigma_0 l' [\phi(t') - \phi(t)] \tag{59a}$$

where σ_0 denotes the shear stress over the layer. Taking the limit of $\Delta t = t' - t \to 0$, we find:

$$\dot{\gamma}(t) = \sigma_0 l(t) \dot{\phi}(t) \tag{59b}$$

in which a dot denotes differentiation with respect to time t. Since the materials compliance $J(t)$ is supposed to be proportional to $\gamma(t)/\sigma_0$ we find from equation (59b):

$$\dot{J}(t) = k l(t) \dot{\phi}(t) \tag{59c}$$

in which k is a proportionality constant.

At (loading) time t, the time elapsed after quenching has increased from t_e (moment of loading) to $t_e + t$.

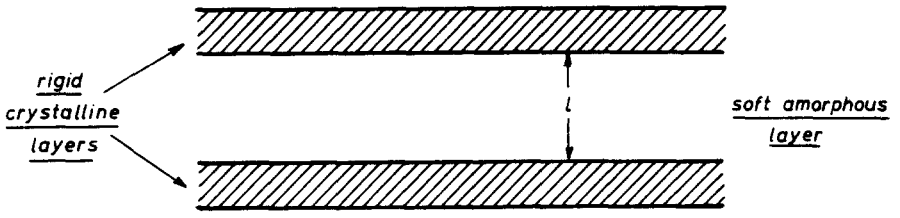

Figure 22 Model for explaining the smallness of the effect of secondary crystallization on the long term creep. For details see text

Therefore:

$$l(t)=l_{t_e}\left[1-\frac{B}{2.303}\ln(1+t/t_e)\right] \tag{60}$$

Let us compare $J(t)$ with the compliance $J^*(t)$ that would be obtained when l remained constant and equal to l_{t_e}. We have:

$$J^*(t)=kl_{t_e}\phi(t)>J(t)=kl(t)\phi(t) \tag{61}$$

Combining equations (59)–(60) we obtain:

$$\dot{J}^*(t)-\dot{J}(t)=(kl_{t_e}B/2.303)\ln(1+t/t_e)\dot{\phi}(t) \tag{62}$$

Dividing by $J^*(t)$ and changing to $\ln t$ derivatives we find:

$$\frac{1}{J^*}\frac{\mathrm{d}[J^*-J]}{\mathrm{d}\ln t}=\frac{B}{2.303}\ln(1+t/t_e)\frac{\mathrm{d}\ln\phi}{\mathrm{d}\ln t} \tag{63}$$

Because of equation (61), $\mathrm{d}\ln\phi/\mathrm{d}\ln t$ is equal to $\mathrm{d}\ln J^*/\mathrm{d}\ln t$.

By writing m for this double logarithmic rate, we find:

$$\frac{1}{J^*}\frac{\mathrm{d}[J^*-J]}{\mathrm{d}\ln t}=\frac{Bm}{2.303}\ln(1+t/t_e) \tag{64}$$

Parameters B and m can be estimated from the experimental data. From Figure 20 of ref. 2 we obtain a B value of -0.09 at 20°C (9%/decade). Slope m can be determined from *Figure 20* of the present paper. In the flat long time part, J shows a slope of about 10%/decade, i.e. $m=0.1/2.303=0.043$. Consequently, $Bm/2.303$ equals 0.0017 and for $t<300t_e$ (see *Figures 20* and *21*), we obtain:

$$\frac{1}{J^*}\frac{\mathrm{d}[J^*-J]}{\mathrm{d}\ln t}<0.01 \tag{65}$$

We thus find that the slopes of $J^*(t)$ and $J(t)$ *versus* $\ln t$ do not differ by more than 1%. For $t\ll t_e$, J^* and J are equal. Let us say that $J^*=J$ for $t=0.1t_e$. Since $t<300t_e$, this implies that the variation in $\ln t$ is limited to a factor $\ln 3000=8$. So, the differences between J^* and J will be less than 8%.

The physical meaning of this result is easily understood. If m is small, the major part of the deformation is built up during the earlier stages of creep, i.e. for $t<t_e$. For $t>t_e$, the stress on the rubbery amorphous material as well as the properties of the rubber remain constant. Therefore the crystallization process does not change the deformation built up for $t<t_e$; it only reduces the rate of creep for $t>t_e$. Consequently, the differences between the two compliances will be proportional to the product of m and B. If m were zero, the differences would also be zero.

DISCUSSION

The previous sections have indicated how the long term creep of semi-crystalline polymers can be predicted from short-time tests. In region 1, we can apply the methods developed for amorphous polymers (the effective time method, or the linear extrapolation method). In regions 2 and 3 we can use the modified effective time method, or again a linear extrapolation method, and in region 4 we can apply time–temperature superposition.

One remark, however, should be made. Just as for amorphous polymers we have now demonstrated the accuracy of the prediction methods on our laboratory time scale of 1000 h. For amorphous polymers we could safely conclude (page 127 of ref. 1) that, because the method correctly predicts the 1000 h behaviour from a 1 h test, it will equally well predict the behaviour over 10^5 h (10 years) from a test of 100 h. For crystalline polymers, such a conclusion is less certain.

The reasons for this become clear when we consider the behaviour of PE. Its α peak has a rather low activation energy, and therefore, the transition to region 4 may rapidly shift to lower temperatures with increasing creep time. So, it is not certain whether the creep of, for example, HDPE at 20°C which is of type 3 at short times, will remain of type 3 for times of the order of years. The behaviour may change to type 4, and this may upset the predictions, although in such cases, the actual creep will be less than predicted, i.e. the prediction will be on the safe side. Clearly, these points have yet to be clarified by very long creep tests. A more detailed discussion of this problem is given in reference 14.

CONCLUSION

The methods for predicting long term creep from tests of short duration, previously developed for amorphous polymers, can also be used in a slightly modified form for semi-crystalline polymers.

ACKNOWLEDGEMENTS

The author wishes to acknowledge Akzo, ANIC, BP-Chemicals, DSM, Chem.-Werke Hüls, Montedison, Rhône-Progil and Shell for sponsoring the work during the years 1973/74 when most of the results reported here were obtained. Moreover, he is greatly indebted to Mrs C. Zoeteweij and Mrs M. P. Bree for carefully performing the experiments.

REFERENCES

1 Struik, L. C. E. 'Physical Aging of Amorphous Polymers and Other Materials', Elsevier, Amsterdam, 1978
2 Struik, L. C. E. *Polymer* 1987, **28**, 1521

3 Struik, L. C. E. *Polymer* 1987, **28**, 1534
4 Willbourn, A. H. *Trans. Faraday Soc.* 1958, **54**, 717
5 Heijboer, J. *Br. Polym. J.* 1969, **1**, 3
6 McCrum, N. G., Read, B. E. and Williams, G. 'Anelastic and Dielectric Effects in Polymeric Solids', Wiley, London, 1967
7 Hopkins, I. L. *J. Polym. Sci.* 1958, **28**, 631
8 Haugh, E. F. *J. Appl. Polym. Sci.* 1959, **1**, 144
9 Staverman, A. J. and Schwarzl, F. R. in 'Die Physik der Hochpolymeren', Vol. IV (Ed. H. A. Stuart), Springer, Berlin, 1956
10 Struik, L. C. E. in 'Failure of Plastics' (Eds. W. Brostow and R. D. Corneliussen), Hanser, Munich, 1986, p. 220
11 Moore, D. R. and Turner, S. *Plastics and Polymers* 1974, 41
12 Buckley, C. P. and McCrum, N. G. *J. Mater. Sci.* 1973, **8**, 928
13 Kovacs, A. J. Thesis, Faculty of Science, Paris, 1954
14 Struik, L. C. E. *Polymer* 1989, **30**, 815